euspen's 22nd International Conference & Exhibition, Geneva, CH, May/June 2022
www.euspen.eu

Automation development using a digital approach in prototype pipework

Toa Pecur [1], Nan Yu [1], Andrew Sherlock [1, 2], Frank Mill [1]

[1] *Institute of Materials and Processes, School of Engineering, University of Edinburgh, EH9 3FB, Edinburgh, Scotland, UK*
[2] *National Institute for Manufacturing Scotland*

toa.pecur@ed.ac.uk

Abstract
Commonplace methods for measuring large assemblies that are prone to change have revolved around manual measurements. There is an increasing need for utilising the data in a digital format by capturing a digital shadow of the physical model. By doing so would expedite compliance checking of potential conflicting parts earlier in the manufacturing processes found in large scale metrology. Oftentimes, this would entail an intact 3D point cloud scan, or in the case of partial scans a varied amount of operator steps to deduce the characteristics captured by a scanner. This work aims to streamline and automate a section of this process enabling more fluid dimensioning of the pipe components within a scaled-down physical prototype pipeline model.

Keywords: large scale metrology, point clouds, prototype pipework, as-built to as-designed

1. Introduction

Manual operator work when measuring and dimensioning components has been susceptible to drawn-out times as well as, occasional human errors when measuring and reverse engineering parts from their as-built components. This is an active area of research for automation of components found within the scene, together with pipeline contributions spanning from the build environment [1,2] to the shipbuilding setting [3]. This work aims to increase the flexibility of segmentation, introducing computer aided design (CAD) parts into the scene to aid compliance checking when working with partial scans.

In this workflow we use non-contact based measurements to compare the as-designed to the reference design in addition to using minimum a priori from the scene to segment pipe sections.

2. Methodology

A physical pipeline prototype model (3PM) shown in Figure 1 and its corresponding CAD model was created for comparisons. The individual pipes have an outer diameter of 36 mm and a length depending on the translational movement allowed within the box. In total, there are nine different lengths of pipes and six similar 45° elbows within the scene.

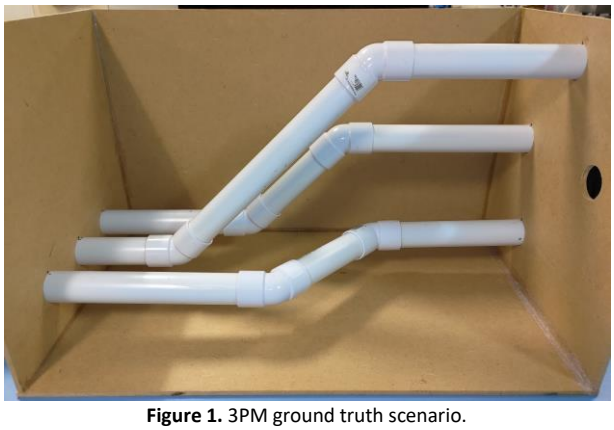

Figure 1. 3PM ground truth scenario.

2.1. Preprocessing

A scan using a FaroArm laser line probe was carried out on the 3PM with a scanning error of 0.0207 mm which has been compensated beforehand. The scan was completed in one sitting to simulate a quicker scan that would be carried out by an operator where partial views and missing information from areas are obtained. After the point cloud scan was obtained, an octree downsampling is performed reducing the points from 55 million to 1 million for further processing.

Random sample consensus (RANSAC) [4] of a plane is used to segment the four main sides found around the 3PM. Noise filtering via the statistical distance of the points compared to the mean in the point cloud is required to further clean spurious points left over from the segmentation. Density-based spatial clustering of applications with noise (DBSCAN) [5] is performed to enable the three different segments of pipes (A, B, and C) to be grouped individually seen labelled in Figure 2. The world origin is centred around segment B at the base of the pipe section seen below with green corresponding to y axis, blue z axis, and red for the x axis, the same origin is used in the CAD assembly.

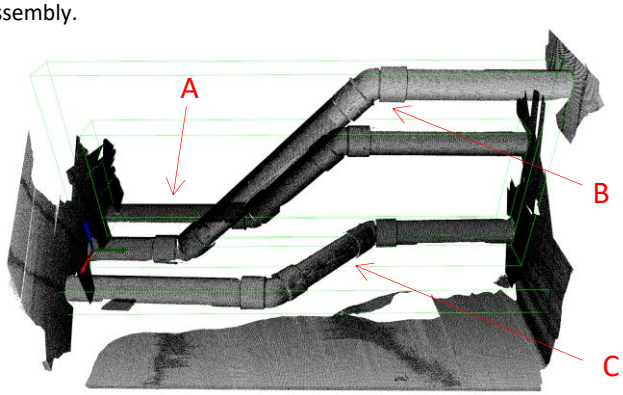

Figure 2. Clustered point cloud with axis aligned bounding boxes around the three segments.

2.2. Fitting

The three clusters obtained previously undergo a registration-like step where the elbow is segmented from each of the three clusters separately. Firstly, fast point feature histogram (FPFH) local descriptor [6] is computed for all three segments of the

clusters as well as, the elbow model with roughly the correct coordinates in space obtained from the CAD. The elbow is then registered to the segments with a defined threshold allowing for movement of the initial placement utilising RANSAC. Once the registration converges, the nearby points from the elbow model are removed from the segment, as seen in Figure 3.

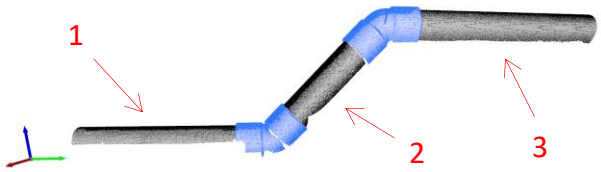

Figure 3. Segment A cylindrical sections (gray points) segmented by removing elbows (blue points).

Next, these points from segment A are clustered to correspond to three different cylindrical sections. Oriented bounding boxes (OBB) and axis aligned bounding boxes (AABB) are computed for all the cylinders with AABB seen in Figure 4.

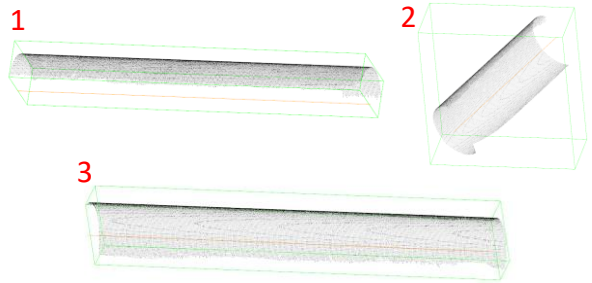

Figure 4. Segment A cylinders where AABB = green and centreline = orange.

The difference of angles between the axis of each cylinder is computed relative to the XY, YZ, and XZ planes creating a new local axis which is rotated around the differences of the angles for each cylinder box. These cylinder sections are further divided into smaller slices for fitting circles along the length of the cylinder.

Algebraic circle fitting by Taubin [7] has been deployed for the individual sliced sections. It has been reported that the fitting was done with good performance relative to Pratt and Kasa algebraic fits [8]. Input parameters are not required for algebraic fits, allowing a range of different sized cylinders in the future to be acquired without specifying the individual sizes. The circle is fitted onto the XZ plane with the general equation seen below:

$$(x + a)^2 + (z + b)^2 = r^2 \quad (1)$$

Where a and b correspond to the x and z circle centres and r is the radius of the plotted circle.

3. Results

The procedure provided accurate segmentation results for the cylinders (pipes), as well as accurate positioning of the cylinder centres (Figure 4) and radii (Figure 5) for segment A. Cylinder two is observed to contain the lowest deviations of the circle fits, attributed mainly to the higher partial surface area scanned when compared to the other partial cylinder scans observed in Figure 5. Nonetheless, cylinder one and three circle fits proved to be accurate with acceptable deviations.

Segment A cylinder sections have a length of 171.420 mm σ = 0.032 mm, 98.183 mm σ = 0.083 mm, and 206.270 mm σ = 0.082 mm for one, two, and three respectively from their end points. Compared to the CAD values, 170 mm, 100 mm, 205.75 mm for cylinder one, two, and three.

Both cylinder one and three centrelines were observed to contain small angle rotations in respect to their XZ and YZ planes. Where cylinder two was seen to contain a rotation of 1.838° in XZ and 44.846° in YZ plane when compared to the CAD centrelines of 45° in YZ plane and no further rotations.

In addition to the real scanner data, synthetic data was also utilised from a virtual scanner [9] which produced similar segmentation results. The scanning accuracy was kept high, as well as, the noise level was kept low to allow for better fitting accuracy.

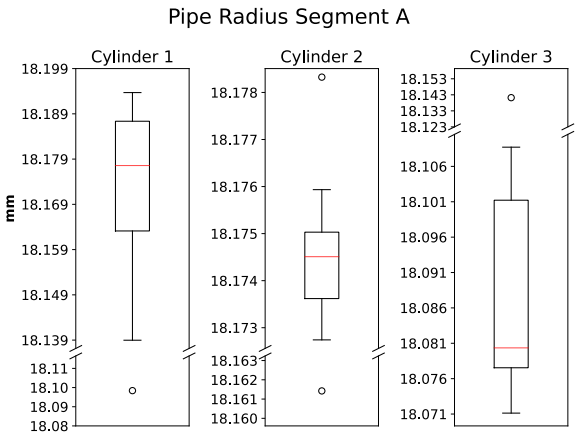

Figure 5. Segment A cylinder radius fitting results.

4. Conclusions

This paper has demonstrated early work in automation for a 3PM digital shadow to aid dimensioning with the help of a reference elbow model. The procedure was applied successfully segmenting components from a point cloud pipeline without user interaction providing radius and length information. Moreover, in the future arbitrary diameter pipes will facilitate easier dimensioning without user input of nominal values. In this work both real and synthetic data was applied for the trialling of the pipeline.

References

[1] A. K. Patil, P. Holi, S. K. Lee, and Y. H. Chai, 2017, *Autom. Constr.*, An adaptive approach for the reconstruction and modeling of as-built 3D pipelines from point clouds, **vol. 75**, 65–78

[2] K. Kawashima, S. Kanai, and H. Date, 2014, *J. Comput. Des. Eng.* As-built modeling of piping system from terrestrial laser-scanned point clouds using normal-based region growing, **vol. 1**, no. 1, 13–26,

[3] R. Moritani, S. Kanai, H. Date, M. Watanabe, T. Nakano, and Y. Yamauchi, 2018, *Comput. Aided. Des. Appl.*, Cylinder-based simultaneous registration and model fitting of laser-scanned point clouds for accurate as-built modeling of piping system, **vol. 15**, no. 5, 720–733

[4] M. A. Fischler and R. C. Bolles, 1981, *Graph. Image Process.*, Random Sample Paradigm for Model Consensus: A Apphcatlons to Image Fitting with Analysis and Automated Cartography, **vol. 24**, no. 6, 381–395

[5] M. Ester, H.-P. Kriegel, J. Sander, X. Xu, 1996, *in kdd*, A density-based algorithm for discovering clusters in large spatial databases with noise., **vol. 96**, no. 34, 226–231.

[6] R. B. Rusu, N. Blodow, and M. Beetz, 2009, *Proc. - IEEE Int. Conf. Robot. Autom.*, Fast Point Feature Histograms (FPFH) for 3D Registration, 3212–3217

[7] G. Taubin, 1993, *Int. Conf. Comput. Vis.*, An improved algorithm for algebraic curve and surface fitting, 658–665

[8] A. Al-Sharadqah and N. Chernov, 2009, Electron. J. Stat., Error analysis for circle fitting algorithms, **vol. 3**, 886–911

[9] L. Winiwarter et al., 2022, *Remote Sens. Environ.*, Virtual laser scanning with HELIOS++: A novel take on ray tracing-based simulation of topographic full-waveform 3D laser scanning, **vol. 269**